ELECTRO-OPTIC MODULATOR BASED ON ORGANIC PLANAR WAVEGUIDE INTEGRATED WITH PRISM COUPLER

Summary of research

Principal Investigator: Dr. Sergey S. Sarkisov

Period: June 1, 1999 to May 30, 2002

Alabama Agricultural and Mechanical University
Office of Research and Development
4900 Meridian Street, P.O.Box 1057, Normal, Alabama 35762
Telephone: 256-851-5675, Fax: 256-851-5030

NASA Grant NAG8-1498

Associate research personnel

A. Principal investigator

Dr. Sergey Sarkisov

B. Research faculty

Dr. Michael Curley

C. Graduate students

1. Curtis Banks
2. Darnell Diggs
3. Zhifu Liu
4. Aisha Fields
5. William Omereji
6. Daniel Wilson

D. Undergraduate students

1. William Omereji
2. Thomas Graham

Subcontractor

Dr. Alex Leyderman, University of Puerto Rico in Mayaguez

Table of contents

1. Objectives and accomplishments

The objectives of the project, as they were formulated in the proposal, are the following.

- Design and development of novel electro-optic modulator using single crystalline film of highly efficient electro-optic organic material integrated with prism coupler
- Experimental characterization of the figures-of-merit of the modulator. It is expected to perform with an extinction ratio of 10 dB at a driving signal of 5 V
- Conclusions on feasibility of the modulator as an element of data communication systems of future generation

The accomplishments of the project are the following.

- The design of the electro-optic modulator based on a single crystalline film of organic material NPP has been explored. The problems of building a version of the modulator integrated with prism coupler have been identified. Preliminary testing of thin film waveguide prototype of the modulator has been performed.
- The evaluation of the figures-of merit of the electro-optic modulator has been performed. It is based on the characterization of the electro-optic properties of the films using the longitudinal intensity modulation technique with low (of the order of 10 V) alternating driving voltage. Both the fundamental and double frequency responses were used for the characterization. The electro-optic effect was pseudo longitudinal since the configuration of the experiment was that of a longitudinal intensity modulator but the main contribution to the effect originates from the transverse component of the external electric field. By purely electro-optic means we determined the orientation of the dielectric axes and measured the half-wave voltage, the figure-of-merit, and electro-optic coefficients r_{12} and r_2 to be 3.24 kV, 99.2 pm/V, 461 pm/V, and 154 pm/V respectively. We also found that electro-optic coefficients r_{61} and r_{63} were two orders of magnitude less than r_{12} and r_2. Respectively, the driving voltage of the modulator in the transverse waveguide

configuration would be 3.24 V (the length of the waveguide is assumed to be 10 mm and the thickness of the single crystal film – 10 μm). The extinction ratio of the experimental modulator in the pseudo longitudinal configuration (Fig. 7) was approximately 8.4 dB, slightly less than expected. The improvement of the extinction ratio could be expected in the next generation of the modulator with higher optical quality of the single crystal films grown.

- Based on the results of characterization of the figures-of merit, the conclusion was made that the modulator based on a thin film of NPP is feasible and has a great potential of being used in optic communication with a modulation bandwidth of up to 100 GHz and a driving voltage of the order of 3 to 5 V.

Comparison of the objectives and the achievements shows that all the objectives of the project outlined in the initial proposal have been met.

2. Motivation

Organic crystalline materials with large electro-optic (E-O) effect are favorable candidates for fast E-O modulators because of their substantially low dispersion of E-O coefficients comparing to conventional inorganic E-O materials such as $LiNbO_3$ and KDP.[1] Large E-O coefficients have been recently reported for 2-methyl-4-nitroaniline (m-NA)[2], N-(4-nitrophenyl)-(L)-prolinol (NPP)[3], and 4-N,N-dimethylamino-4'-methyl-stilbazolium tosylate (DAST).[4] Introduction of these materials into integrated optical devices requires preparation of thin films in monocrystalline form. Growth of single crystal films of NPP has already been reported [3,5] but the characterization of E-O properties of such films was done only when the external electric field was oriented along the plane of the film and across the propagation direction of the light beam (transverse E-O modulator). The characterization of E-O properties of NPP films was done in longitudinal configuration, when the electric field is applied across the film and along the propagation direction of light. The linear E-O effect, though quite significant, is still a result of contribution from the transverse component of the field and can be called as pseudo longitudinal. The report also describes the growth of single crystal films of NPP

by the plate-guided method and the results of measurements of the half-wave voltage, the figure-of-merit, and E-O coefficients r_{12}, r_{22}, and r_{63}.

3. Material selection and sample preparation

Bulk crystal of NPP was grown by the group of J. Zyss in 1984.[5] NPP belongs to monoclinic crystal class, and its space group is $P2_1$. Its tensor of E-O coefficients is

$$\begin{bmatrix} 0 & r_{12} & 0 \\ 0 & r_{22} & 0 \\ 0 & r_{32} & 0 \\ r_{41} & 0 & r_{43} \\ 0 & r_{52} & 0 \\ r_{61} & 0 & r_{63} \end{bmatrix} \quad (1)$$

The bulk crystal is biaxial and its refractive indices n_x, n_y, n_z at 633-nm wavelength are 2.066, 1.876, and 1.478 respectively.[6] The crystal is optically transparent in the range 0.48 to 2 μm. The E-O coefficients r_{12} and r_{22} of NPP in the form of a single crystal film were evaluated in transverse configuration as 65 pm/V and 22 pm/V.[3] Other E-O coefficients are unknown.

Growing relatively large single crystal films of NPP remains a challenging task. There have been reported just few successful results. [7,8] Here we describe a relatively simple approach to growing single crystal films of NPP based on modified Bridgman or the so-called plate-guiding method.[9-11] This approach has such advantages as full control over the thickness of the film and selection of a proper seed for initial crystal growth. Fig. 1 shows the schematic of the cell where the film of NPP was grown. The cell is made of two round quartz plates 1 and 2. Plate 1 is a lid. Plate 2 has a round trough 3 in the center and works as a container for a thin crystal of NPP. The trough is surrounded by a circular trench 4, which collects the excessive material during melting process. The plates have on their inner surfaces Indium Tin Oxide (ITO) electrodes 5 and 6. Gold wires 7 and 8 are attached to the electrodes on opposite sides of the cell. Parameter d is the depth of the trough and correspondingly the thickness of the film. In our experiments

we had d = 10 micron. The cell was mounted on a table of a conventional optical microscope between two crossed polarizers. This was done in order to monitor continuously the growth of the crystal. The table was heated by circulating oil. The heat came to the cell from the side of plate 2 (Fig. 1b). Initially, polycrystalline powder of NPP was put in the trough. Plate 2 was then heated. When the material melted down, plate 1 was mounted. The excess of the melted material was collected in the trench. Then the film was let to cool down. At this stage, the material showed dense polycrystalline structure when observed under the microscope with crossed polarizers (Fig. 2a). In our system the temperature in the middle of the trough was maintained lower than that at the edges. We heated the cell and cooled it down multiple times until we had only one seed in the middle with the rest of the material in the melt. The melt was observed in the microscope as a dark uniform region while the seed was seen as a uniformly illuminated faceted single crystal (Fig. 2b). We then let the melt to cool down slowly and to develop into a single crystal film from the selected seed. By slow cooling the single crystal grew gradually from the melt using the selected seed. Microscope photographs of different parts of a typical single crystal film are presented in Fig. 3. Fig. 3a shows a region consisting of long uniform stripes separated by parallel cracks, and Fig. 3b demonstrates a region with relatively wide uniform area (about 0.36×0.68 mm^2). The size of the latter one is big enough for a laser beam (of 0.5 mm diameter) to pass through it without significant scattering.

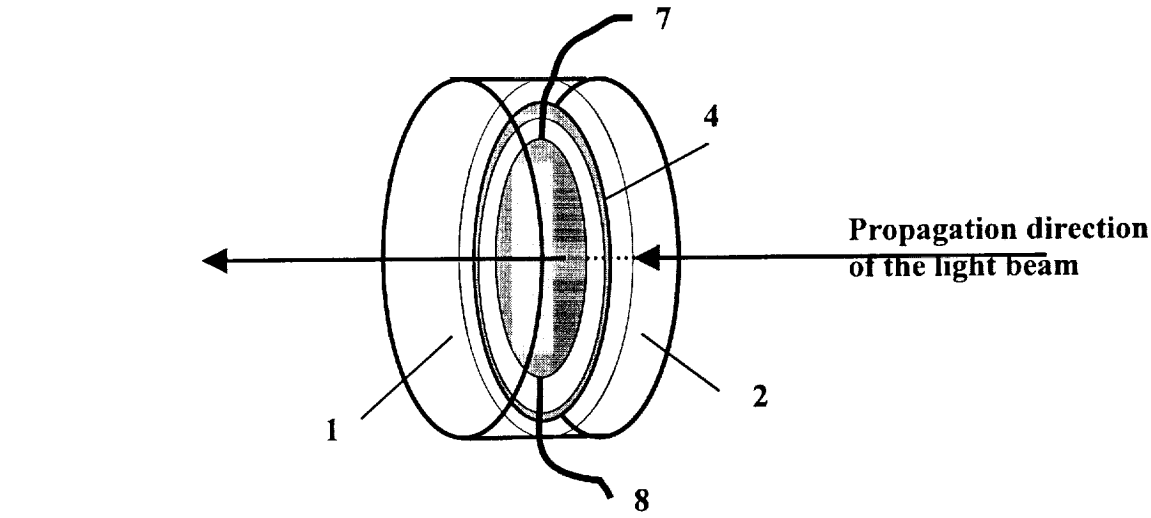

(a)

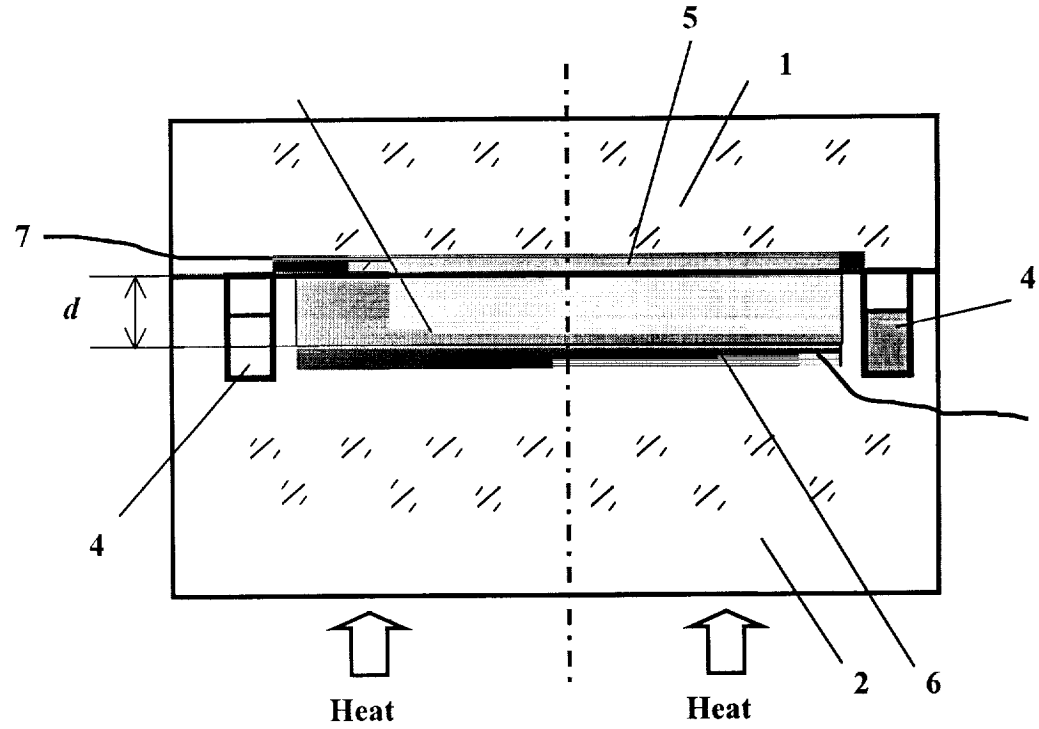

(b)

Fig. 1. Schematic of the cell where single crystal thin film of NPP was grown. The cell is shown (a) as it is oriented with respect to the light beam and (b) in cross-sectional view.

4. Experimental set-up

We characterized the electro-optic properties of thin film samples of NPP using a modified version of the a.c. modulation method proposed by Yoshimura.[12] In this technique characterization could be done with relatively low (of the order of 10 V) a.c. voltage applied to the sample. The experimental setup for characterization of E-O properties of thin film organic crystals in longitudinal mode is shown in Fig. 4. A 35-mW He-Ne laser provides linearly polarized light beam at a wavelength of 633 nm. Mirror M directs the beam to the sample. Then the beam runs through polarizer P_1, the cell with the sample (10-μm thick film of NPP), and polarizer P_2. The cell is mounted on a holder with six degrees of freedom: three translations and three rotations. This provides flexibility in orientation of the sample with respect to the incident light beam. An optic fiber transmits the output light to a photo detector. An a.c. voltage with maximum amplitude of up to 24 V from a signal generator is applied to the electrodes of the cell. The signal from the photo detector is processed by a lock-in amplifier, which is synchronized by the signal generator. An oscilloscope monitors the signal from the photo detector.

(a)

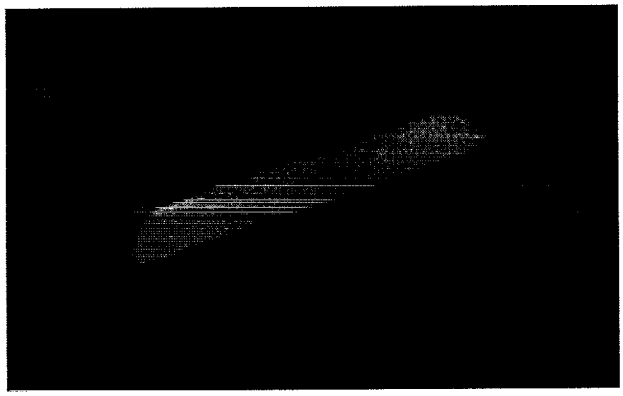

(b)

Fig. 2. A seed used for the growth of single crystals.

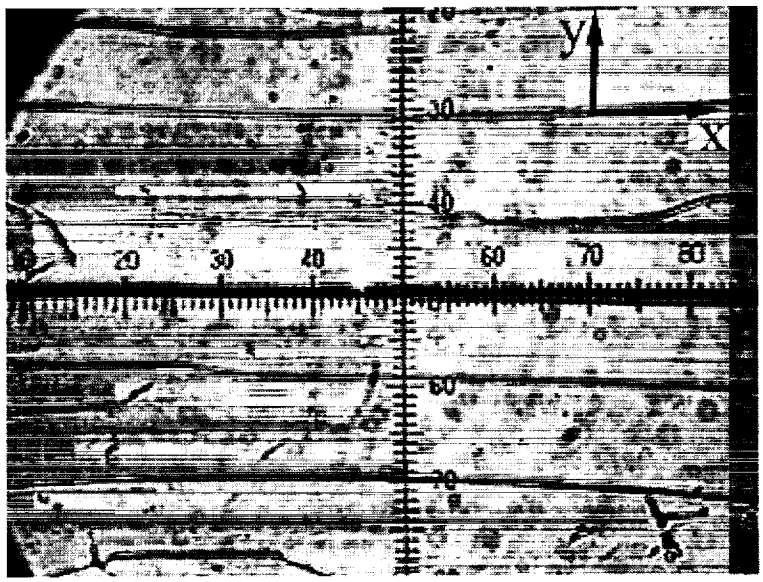

(a)

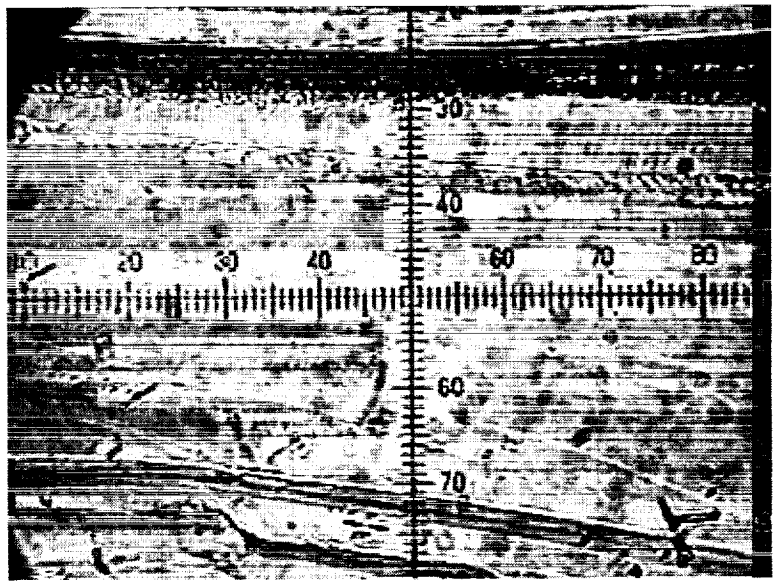

(b)

Fig. 3. The microscope photographs of (a) region of a single crystal of NPP consisting of long uniform stripes, (b) region with relatively wide uniform areas. The size of the main unit of the scale in the photographs is 90 μm.

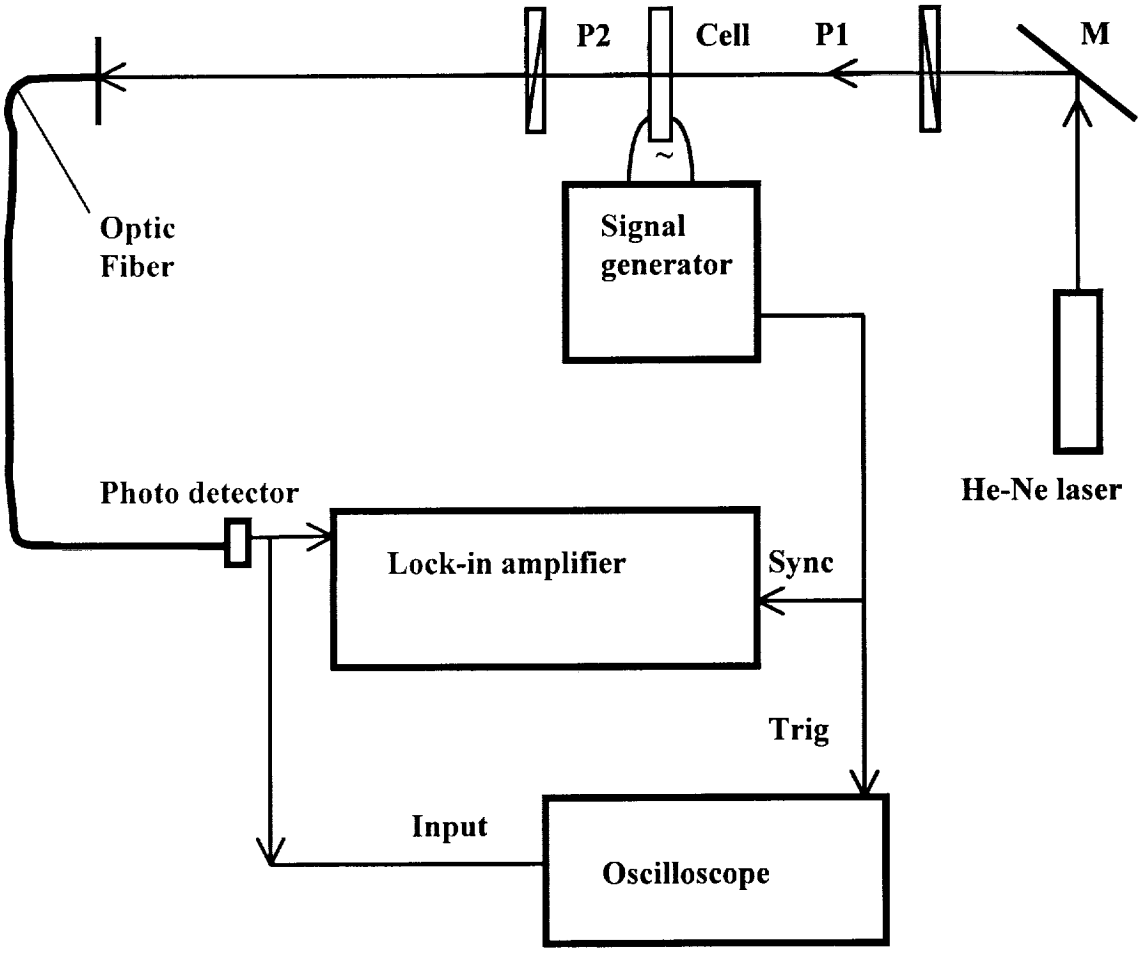

Fig. 4. Experimental setup for characterization of E-O properties of thin film samples. M is the mirror, P_1, P_2 are the polarizers.

Experimental characterization of the E-O properties starts from determining the orientation of dielectric axes. It has been suggested that dielectric axes x and y lay in, and z was normal to the plane of the film.[3] Theoretical analysis shows that if the two-fold axis y is within the plane of the film, the linear E-O effect does not exist at the orientation of the crystal we used in the experiment (see Appendix A). However, our preliminary measurements showed an unexpectedly strong linear E-O effect. Thus the two-fold axis y more likely lay off the plane of the film. We also observed a drop of the intensity of the transmitted light ("dark field") when the sample placed in a polarizing microscope between crossed polarizers was rotated until the cracks became parallel to the polarization direction of either polarizer. One possible explanation is that the cracks were likely oriented along a direction close to the direction of dense packing in the crystal. The latter direction must be parallel to axis x, since n_x is the highest refractive index of NPP. The observation of the "dark field" additionally suggested that this was the case. If the crystal is oriented with axis x parallel to either polarizer, the light passing through it remains linearly polarized along the direction of the input polarizer and thus can not pass through the cross-oriented output polarizer. The two above-mentioned experimental facts allowed us to assume that even if the plane made by the pair of axes x and y lay off the plane of the film, the tilt was not substantial. In other words, the angle between axis z and the normal to the film was more likely of the order of few degrees. In fact, our detailed investigation (Appendix B) showed that this angle was only 5.2^0. The maximum of the E-O effect had to be observed when the light propagated along axis z.

5. Theory

Accordingly, in further description of the experimental approach we always assume the optimum orientation of the film at which the propagation direction of the light is parallel to axis z. This configuration is shown in Fig. 5. The angle between axis z and the normal to the film w is denoted as ξ. The projection u of axis x on the plane of the film is parallel to the cracks. During observations of the E-O effect polarization direction P_2 of the output polarizer was always kept at an angle of 90^0 with respect to polarization direction P_1 of the input polarizer. The angle between axis x and P_1 is denoted as θ. It is

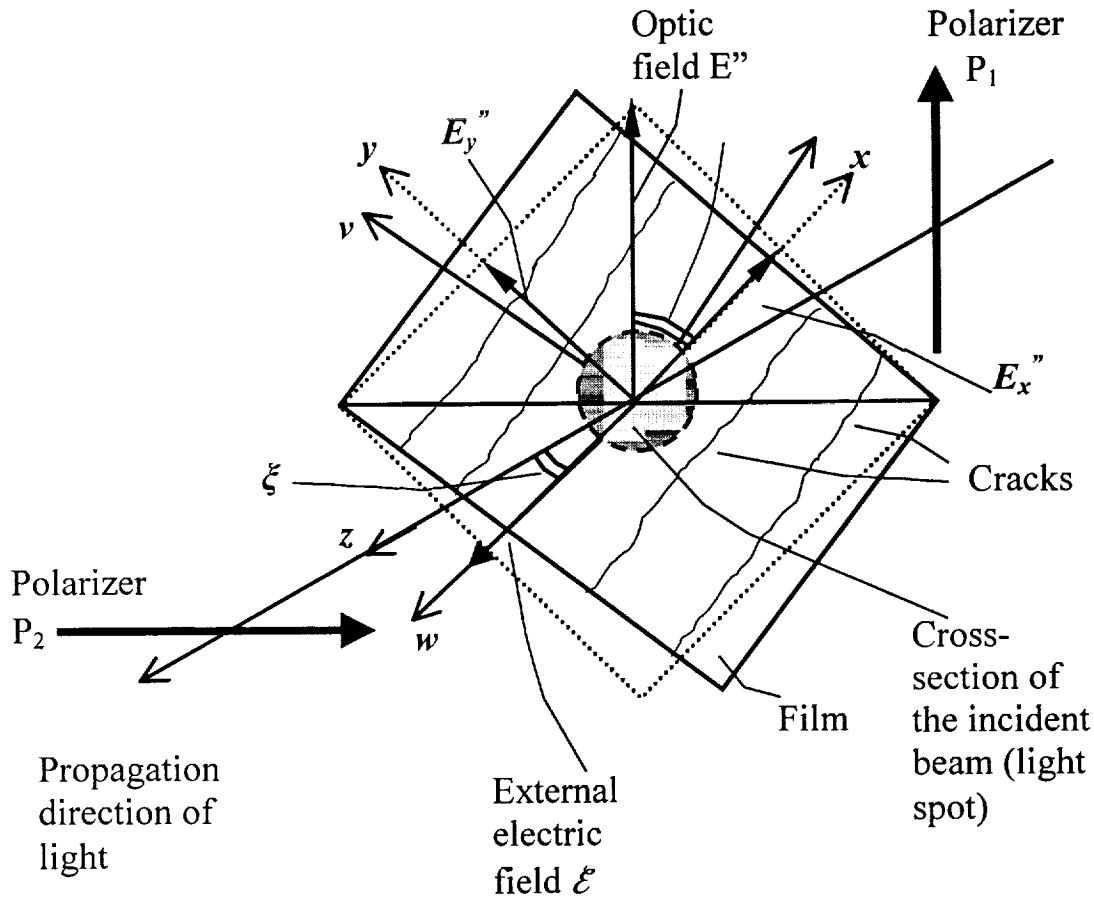

Fig. 5. The configuration of the polarization directions of input polarizer P_1 and output polarizer P_2 and the orientation of the optic axes of the crystalline film of NPP. E'' is the optic field after passing polarizer P_1.

important to mention that the optimum orientation of the film corresponded to $\theta \approx 45^0$ (Fig. 5).

Below we provide the derivation of the equations, which link the E-O parameters of the film, such as the half-wave voltage, the figure-of-merit, and the E-O coefficients, to the experimental data.

After passing polarizer P_1, the light beam is vertically polarized. The magnitudes of x and y components of optic field ***E"*** (Fig. 5) are

$$E_x'' = E_0 \cos\omega t \cos\theta, \tag{2}$$

$$E_y'' = E_0 \cos\omega t \sin\theta, \tag{3}$$

where E_0 is the amplitude of the optic field, ω is the angular frequency of light. The linearly polarized light then runs through the sample. The effective distance, which the light travels within the crystal, is

$$d_{eff} = d/\cos\xi, \tag{4}$$

where d is the thickness of the film. Now we have to find the refraction, which the optic field experiences within the crystal.

The anisotropy of refraction of a biaxial crystal like NPP with no external electric field applied is described by the ellipsoid of refractive indices

$$x^2/n_x^2 + y^2/n_y^2 + z^2/n_z^2 = 1. \tag{5}$$

We implement E-O modulation by applying an alternating voltage to the electrodes on both sides of the film (Fig. 1). The voltage can be described by formula

$$V_a(t) = V_0 \cos\Omega t, \tag{6}$$

where V_0 is the amplitude, Ω is the angular frequency. The alternating external electric field $\mathcal{E}$ created by the voltage is normal to the film (Fig. 5). Its magnitude can be described as

$$\mathcal{E}(t) = V_a(t)/d = \mathcal{E}_0 \cos\Omega t, \tag{7}$$

where $\mathcal{E}_0 = V_0/d$ is the amplitude. Since the external field is not parallel to axis z and respectively to the direction of light propagation, in addition to the longitudinal component $\mathcal{E}_z$(t), it has also non- zero transverse components $\mathcal{E}_x(t)$ and $\mathcal{E}_y(t)$:

$$\mathcal{E}_x(t) \approx \mathcal{E}(t) \cos 45^0 \sin\xi = (V_0/d) \cos 45^0 \sin\xi \cos\Omega t\,, \tag{8}$$

$$\mathcal{E}_y(t) \approx \mathcal{E}(t) \sin 45^0 \sin\xi = (V_0/d) \sin 45^0 \sin\xi \cos\Omega t\,, \tag{9}$$

$$\mathcal{E}_z(t) = \mathcal{E}(t) \cos\xi = (V_0/d) \cos\xi \cos\Omega t\,. \tag{10}$$

The external a.c. electric field $\mathcal{E}$ modifies the ellipsoid of the refractive indices due to the E-O effect. The modified ellipsoid can be described by equation

$$\begin{aligned} &x^2/n_x^2 + r_{12}\,\mathcal{E}_y(t)\,x^2 + y^2/n_y^2 + r_{22}\,\mathcal{E}_y(t)\,y^2 + z^2/n_z^2 + r_{32}\,\mathcal{E}_y(t)\,z^2 \\ &+ 2[r_{61}\,\mathcal{E}_x(t) + r_{63}\,\mathcal{E}_z(t)]xy + 2[r_{41}\,\mathcal{E}_x(t) + r_{43}\,\mathcal{E}_z(t)]yz \\ &+ 2r_{52}\,\mathcal{E}_y(t)xz = 1. \end{aligned} \tag{11}$$

Assuming $z = 0$, we thus obtain the equation of an ellipse, which describes the birefringence of the crystal for an incident optic field, which propagates along direction z

$$a(t)x^2 + b(t)y^2 + c(t)xy = 1, \tag{12}$$

where

$$a(t) = 1/n_x^2 + r_{12}\,\mathcal{E}_y(t), \tag{13}$$

$$b(t) = 1/n_y^2 + r_{22}\,\mathcal{E}_y(t), \tag{14}$$

$$c(t) = 2[r_{61}\,\mathcal{E}_x(t) + r_{63}\,\mathcal{E}_z(t)] \tag{15}$$

Factor $c(t)$ can be also written as

$$c(t) = c_0 \cos \Omega t, \tag{16}$$

where

$$c_0 = 2(r_{61}\cos 45^0 \sin \xi + r_{63} \cos \xi)(V_0/d)\,. \tag{17}$$

The magnitude of electric field $\mathcal{E}$ in our experiments was of the order of 10^6 V/m. Even if we assume E-O coefficients r_{12}, r_{22}, r_{61}, and r_{63} to be of the order of 100 pm/V, a relatively large number, the magnitudes of $r_{12}\mathcal{E}_y(t)$, $r_{22}\mathcal{E}_y(t)$, $r_{61}\mathcal{E}_x(t)$, and $r_{63}\mathcal{E}_z(t)$ will be of the order of 10^{-4}, much smaller than n_x^{-2} or n_y^{-2} in Eqs. (13) and (14).

We may find now a new coordinate system (x', y') in which Eq. (12) takes its canonical form without the mixed third term.[13] The system is linked to (x, y) by the transformations of rotation

$$x = x'\cos q - y'\sin q, \tag{18}$$

$$y = x'\sin q + y'\cos q, \tag{19}$$

where q is the angle of rotation of new axis x' with respect to axis x given by

$$\tan 2q(t) = \frac{c(t)}{a(t) - b(t)}\,. \tag{20}$$

Equation (12) in the new coordinate system can be written as

$$x'^2/n_{x'}^2 + y'^2/n_{y'}^2 = 1, \tag{21}$$

where

$$1/n_{x'}^2 = a(t)\cos^2 q + b(t)\sin^2 q + c(t)\sin q\cos q, \tag{22}$$

$$1/n_y'^2 = a(t)\sin^2 q + a(t)\cos^2 q - c(t)\sin q\cos q, \tag{23}$$

Using the second-order Taylor series expansion with respect to small parameters $r_{12}\mathcal{E}_y(t)$, $r_{22}\mathcal{E}_y(t)$, $r_{61}\mathcal{E}_x(t)$, and $r_{63}\mathcal{E}_z(t)$ in Eqs. (20), (22), and (23), we can now rewrite Eqs. (22) and (23) in the following manner

$$n_x' \approx n_x - \tfrac{1}{2}\mathcal{E}_y(t) n_x^3 r_{12} - \frac{n_x^3}{8(n_x^{-2} - n_y^{-2})} c^2(t), \tag{24}$$

$$n_y' \approx n_y - \tfrac{1}{2}\mathcal{E}_y(t) n_y^3 r_{22} + \frac{n_y^3}{8(n_x^{-2} - n_y^{-2})} c^2(t). \tag{25}$$

The electric field induced birefringence of the crystal for the incident optic field can be obtained as

$$\begin{aligned}\Delta n(t) &= (n_x'-n_y')-(n_x-n_y) \approx -\tfrac{1}{2}(n_x^3 r_{12} - n_y^3 r_{22})\,\mathcal{E}_y(t) + Fc^2(t) \\ &= -e(t) + Fc^2(t),\end{aligned} \tag{26}$$

where factor

$$F = -\frac{(n_x^3 + n_y^3)}{8(n_x^{-2} - n_y^{-2})} \approx 36.3, \tag{27}$$

and term

$$e(t) = \tfrac{1}{2}(n_x^3 r_{12} - n_y^3 r_{22})\,\mathcal{E}_y(t) = e_0 \cos \Omega t, \tag{28}$$

where

$$e_0 = \tfrac{1}{2}(n_x^3 r_{12} - n_y^3 r_{22})(V_0/d)\sin 45^0 \sin \xi. \tag{29}$$

The related phase retardation between the cross-polarized components of the incident optic field can be obtained as

$$\begin{aligned}\delta(t) &= \Phi(n_x - n_y) + \Phi\Delta n(t) + \delta_c' \\ &= \Phi(n_x - n_y) + \delta_c' - \Phi e(t) + \Phi F c^2(t) = \delta_c + \delta_a(t),\end{aligned} \tag{30}$$

where

$$\Phi = 2\pi d_{eff}/\lambda, \tag{31}$$

δ_c' is the unknown constant phase retardation associated with various sources such as birefringence of loaded quartz plates (which we were able to observe with a polarizing microscope), etc., and δ_c is the total constant retardation

$$\delta_c = \Phi\,(n_x - n_y) + \delta_c' \tag{32}$$

Parameter $\delta_a(t)$ in Eq. (30) is the alternating retardation induced by the external field (applied voltage),

$$\delta_a(t) = -\,\Phi\, e(t) + \Phi\, Fc^2(t) \approx -\delta_1 \cos \Omega t + \delta_2 \cos^2 \Omega t, \tag{33}$$

where

$$\delta_1 = \Phi\, e_0 = SV_0\,, \quad \delta_2 = \Phi\, Fc_0{}^2, \tag{34}$$

$$S = (\pi/\lambda)\sin 45^0 \tan\xi (n_x{}^3 r_{12} - n_y{}^3 r_{22}). \tag{35}$$

The first term in the right part of Eq. (33) is the component of the alternating retardation, which is linearly proportional to the external electric field and oscillates at fundamental frequency Ω. By definition, the half-wave voltage V_π is the value of V_0 that makes amplitude δ_1 equal to π. Assuming $\delta_1 = \pi$ and $V_0 = V_\pi$, from Eq. (34) we obtain

$$V_\pi = \pi/S. \tag{36}$$

Substituting V_π into Eq. (34), we can write

$$\delta_1 = \pi V_0 / V_\pi. \tag{37}$$

The half-wave voltage V_π depends on the wavelength λ of the light, as could be seen from Eqs. (36) and (35). The dependence on λ can be excluded in the figure-of-merit of E-O modulation defined as[12]

$$Q = \lambda/(2V_\pi) = \lambda S/(2\pi). \tag{38}$$

In our analysis of refraction we have also to account for the rotation of the ellipse of refractive indices at angle $q(t)$ (Eqs.(18) through (20)). This can be done by redefining the cross-polarized components of the incident optic field (Eqs. (2) and (3)) in the new coordinate system (x', y'). They can be described as

$$E_{x'}'' = E_0 \cos[\theta - q(t)]\cos\omega t, \tag{39}$$

$$E_{y'}'' = E_0 \sin[\theta - q(t)]\cos\omega t. \tag{40}$$

The components of the optic field after passing through the crystal can be obtained as

$$E_{x'}' = E_0 \cos[\theta - q(t)]\cos\omega t, \tag{41}$$

$$E_{y'}' = E_0 \sin[\theta - q(t)]\cos[\omega t + \delta(t)]. \tag{42}$$

The optic field after polarizer P_2 is given by

$$\begin{aligned} E(t) &= E_{x'}' \sin[\theta - q(t)] - E_{y'}' \cos[\theta - q(t)] \\ &= E_0 \sin\{2[\theta - q(t)]\} \sin[\delta(t)/2] \sin[\omega t + \delta(t)/2]. \end{aligned} \tag{43}$$

The intensity detected by the photo detector is

$$I(t) = \langle EE^* \rangle = (1/2)E_0^2 \sin^2\{2[\theta - q(t)]\} \sin^2[\delta(t)/2], \tag{44}$$

where <...> means time averaging performed by the photo detector.

Now we expand $I(t)$ into the second-order Taylor series with respect to small parameters $\delta_a(t)$ and $q(t)$ as

$$I(t) \approx (1/2)E_0^2 \sin^2 2\theta \sin^2(\delta_c/2)\{1+[\cot(\delta_c/2)\ \delta_a(t)-4\cot 2\theta\, q(t)] \\ +[(1/4)\cos\delta_c \sin^{-2}(\delta_c/2)\ \delta_a^2(t)+4\cos 4\theta \sin^{-2} 2\theta\, q^2(t) \\ -2\cot 2\theta \cot(\delta_c/2)\ \delta_a(t)\ q(t)]\} \tag{45}$$

The expression for $I(t)$ in Eq. (45) can be significantly reduced if $\theta = 45^0$, as was the case in our experiment (see Fig. 5). The expression for $I(t)$ thus turns into

$$I(t) \approx (1/2)E_0^2 \sin^2(\delta_c/2)\{1+\cot(\delta_c/2)\ \delta_a(t)+(1/4)\cos\delta_c \sin^{-2}(\delta_c/2)\ \delta_a^2(t) - 4\, q^2(t)\} \\ = I_c - I_\Omega \cos\Omega t + I_{2\Omega}\cos 2\Omega t, \tag{46}$$

where I_c is the constant component of the intensity in the absence of the a.c. voltage that can be written as

$$I_c \approx (1/2)E_0^2 \sin^2(\delta_c/2). \tag{47}$$

In Eq. (47) we neglected small contribution to I_c from the terms proportional to $\delta_a^2(t)$ and $q^2(t)$. I_Ω is the amplitude of the first harmonic of the alternating intensity defined as

$$I_\Omega = (1/4)E_0^2 \sin\delta_c \Phi e_0 = (\pi/4)\, E_0^2 \sin\delta_c\, (V_0/V_\pi). \tag{48}$$

Equation (48) indicates that component I_Ω associated with the linear E-O effect in the crystal is actually a result of contribution from the transverse component of field $\mathcal{E}_y(t)$ (see Eqs. (28) and (29)). Though the configuration of the experiment resembles that of the longitudinal E-O modulator, the effect can be called as pseudo longitudinal.

$I_{2\Omega}$ is the amplitude of the second harmonic of the alternating intensity that can be written as

$$I_{2\Omega} = (1/16)E_0^2 \cos\delta_c\,(\Phi e_0)^2$$
$$+ (1/4)E_0^2 \sin(\delta_c/2)[\cos(\delta_c/2)\,\Phi F - \sin(\delta_c/2)\,(n_x^{-2} - n_y^{-2})^{-2}]\,c_0^2$$
$$= (\pi^2/16)E_0^2 \cos\delta_c\,(V_0/V_\pi)^2$$
$$+ E_0^2 \sin(\delta_c/2)[\cos(\delta_c/2)\,\Phi F - \sin(\delta_c/2)\,(n_x^{-2} - n_y^{-2})^{-2}]\,G\,V_0^2, \quad (49)$$

where

$$G = (r_{61}\cos 45^0 \sin\xi + r_{63}\cos\xi)^2 d^{-2}. \quad (50)$$

Intensity I_Ω normalized by I_c can be written as

$$I_\Omega / I_c = K_1 V_0, \quad (51)$$

where factor

$$K_1 = \pi\cot(\delta_c/2)/V_\pi. \quad (52)$$

For normalized intensity $I_{2\Omega}$ we have

$$I_{2\Omega}/ I_c = K_2 V_0^2, \quad (53)$$

where factor

$$K_2 = (\pi^2/8)\cos\delta_c \sin^{-2}(\delta_c/2)\,V_\pi^{-2} + 2\,[\cot(\delta_c/2)\,\Phi F - (n_x^{-2} - n_y^{-2})^{-2}]G. \quad (54)$$

In finding half-wave voltage V_π we used the experimental approach based on Yoshimura's method (Ref. 12), which includes the following steps.

First, we turned the voltage off and obtained δ_c from an additional experiment described below. When $V_a = 0$, the optic field after the crystal can be described as

$$E_x' = E_0 \cos\theta \cos\omega t, \tag{55}$$

$$E_y' = E_0 \sin\theta \cos(\omega t + \delta_c), \tag{56}$$

Components E_x', E_y' can be combined into equation

$$(E_x')^2/A^2 + (E_y')^2/B^2 - 2E_x'E_y'\cos\delta_c/(AB) = \sin^2\delta_c, \tag{57}$$

where $A = E_0 \cos\theta$, $B = E_0 \sin\theta$. Eq. (57) is the equation of an ellipse in (E_x', E_y') coordinate plane and describes the elliptically polarized optical wave after the crystal.

At $\theta = 45^0$ we have $A = B = E_0/\sqrt{2}$. Eq. (57) then becomes

$$(E_x')^2 + (E_y')^2 - 2E_x'E_y'\cos\delta_c = \sin^2\delta_c E_0^2/2. \tag{58}$$

Eq. (58) is the equation of an ellipse with prime axes rotated at an angle of 45^0 with respect to direction P_1. We can rewrite Eq. (58) in coordinate system (e_x', e_y') parallel to the prime axes of the ellipse as

$$(e_x')^2/(e_{max})^2 + (e_y')^2/(e_{min})^2 = 1, \tag{59}$$

where

$$e_x' = \frac{1}{\sqrt{2}}(Ex' + Ey'), \tag{60}$$

$$e_y' = \frac{1}{\sqrt{2}}(-Ex' + Ey'). \tag{61}$$

Parameters e_{max} and e_{min}, the semi-major and semi-minor of the ellipse respectively, can be linked to natural birefringence δ_c as

$$\cos\delta_c = \frac{e_{\max}^2 - e_{\min}^2}{e_{\max}^2 + e_{\min}^2} = \frac{I_{\max} - I_{\min}}{I_{\max} + I_{\min}}, \tag{62}$$

where $I_{max} \propto e_{max}^2$, $I_{min} \propto e_{min}^2$ are the maximum and minimum intensities of the light passing through polarizer P_2 respectively. Parameters I_{max}, I_{min} were found experimentally. At the orientation of the film shown in Fig. 5 and with the a.c. voltage turned off, we rotated polarizer P_2 (initially oriented horizontally) at a full circle and plotted the intensity of the light versus the angle of rotation as is shown in Fig. 6. I_{max} and I_{min} were found as parameters of fitting the experimental data with ellipse (Fig. 6, solid line). They are shown as mutually perpendicular solid vectors in Fig. 6. Then retardation δ_c was calculated using Eq. (62).

The second step was to find factor K_1 by linear fitting experimental plot $I_\Omega / I_c = f_1(V_0)$. Once K_1 was found, the half-wave voltage V_π could be calculated using Eq. (52) with δ_c known.

We also modified Yoshimura's method by adding the measurements of amplitude $I_{2\Omega}$ of the intensity at double frequency. We extracted parameter K_2 by fitting experimental plot $I_{2\Omega}/I_c = f_2(V_0^2)$ with function f_2 described by Eq. (53). With δ_c and V_π already known, we then could estimate the unknown E-O coefficients r_{61} and r_{63} using Eqs. (54) and (50).

6. Experimental results and discussion

6.1 *The half-wave voltage*

Fig. 7 shows a typical oscillogram of the intensity of light passing through the NPP film (solid curve) with the a.c. voltage applied to it (dashed curve). The peak-to-peak value of a.c. voltage was 18 V. The response of the sample is a periodical signal with the frequency of the a.c. voltage. Fig. 8 shows amplitude I_Ω of the intensity plotted versus amplitude V_0 of the a.c. voltage at a frequency of 82.0 kHz. The plot is an indication of an apparent linear E-O effect in the film. By using Yoshimura's method as described above, we found that $\delta_c = (80 \pm 2)^0$ and $V_\pi = (3.24 \pm 0.06)$ kV.

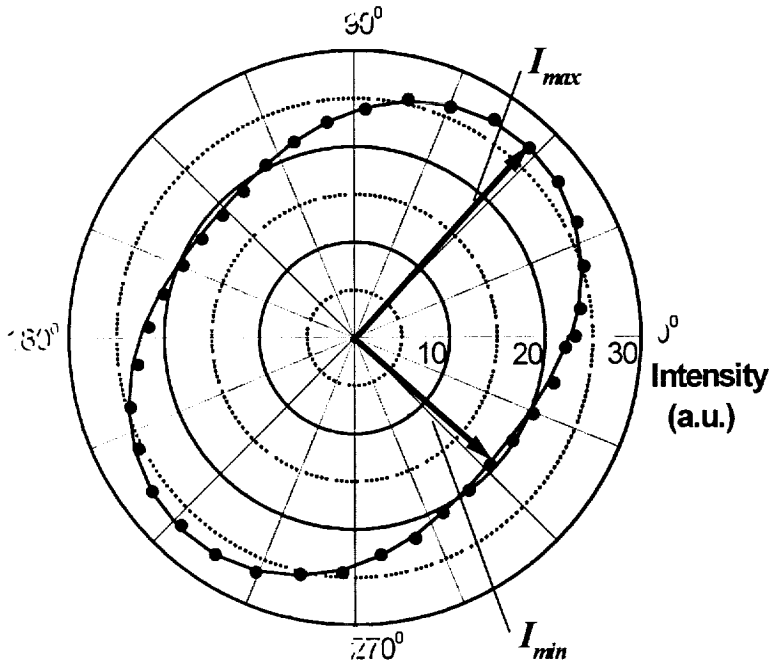

Fig. 6. The intensity of optic field E' after the NPP sample versus the angle of rotation of polarizer P_2 with respect to its initial polarization direction. The polarization direction of P_1 is vertical. The polarization direction of P_2 is initially horizontal. Solid line represents fitting of experimental results.

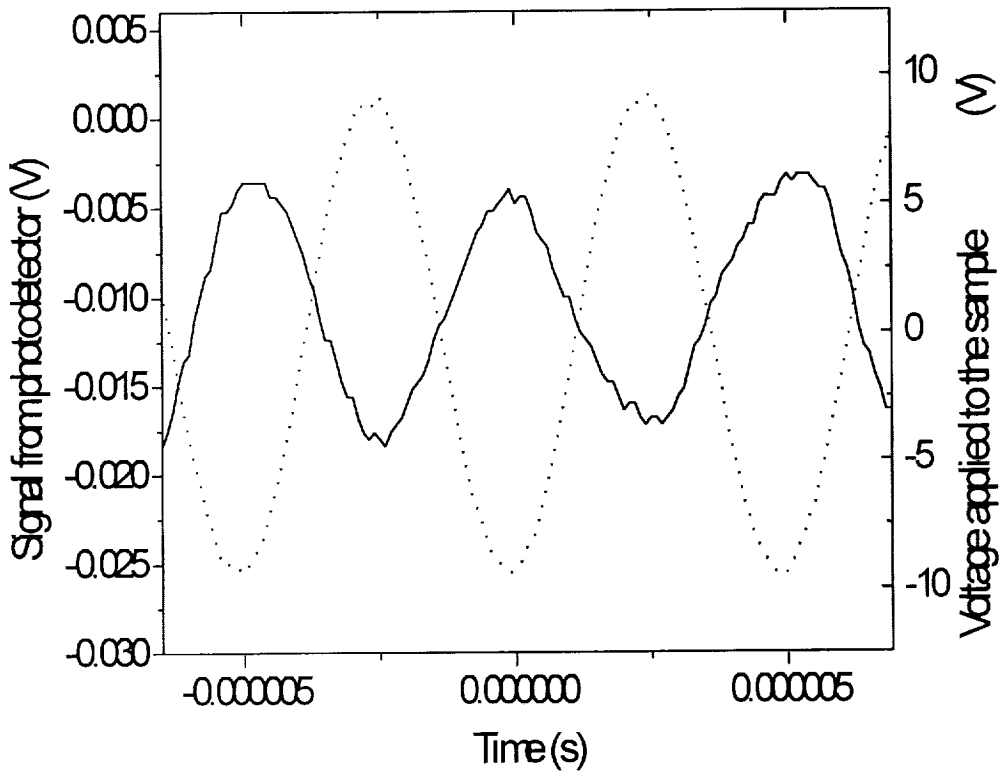

Fig. 7. Oscillogram of the response of the NPP sample (solid curve) to the a.c. voltage (dotted curve) as measured by the photo detector at 200 kHz.

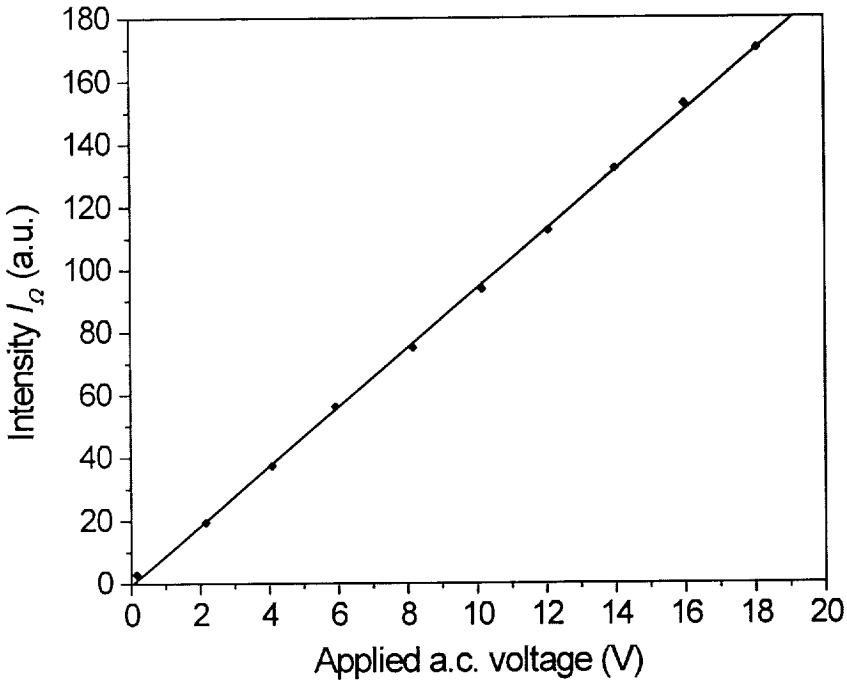

Fig. 8. The amplitude of the signal from the photo detector amplified by the lock-in amplifier versus the amplitude of the a.c. voltage applied to the NPP sample at a frequency of 82.0 kHz. The solid line is linear fitting of the experimental data.

Putting estimated value of V_π in Eq. (38), we calculated the figure-of-merit Q = (99.2 ± 3.4) pm/V, which compares well against that of lithium niobate (about 120 pm/V).[12]

6.2 *Electro-optic Coefficients*

Using previously estimated value of V_π, we were able to obtain E-O coefficients r_{12} and r_{22} from Eqs. (36) and (35). According to Ref. 3, $r_{12} \approx 3r_{22}$. With this assumption in mind, we found coefficient r_{12} and r_{22} to be (461 ± 15) pm/V and (154 ± 5) pm/V respectively. These values are much higher than those reported in Ref. 3. One of the reasons could be the presence of a high internal electric field in the crystal produced by a substantial stress via the conversed piezoelectric effect. The cracks give some evidence to this stress because they can be considered as channels through which the stress had a release.

Fig. 9 displays in logarithmic scale the amplitude of the intensity $I_{2\Omega}$ plotted versus the peak-to-peak value of the a.c. voltage. In accordance with Eq. (53), we approximated experimental data in Fig. 9 with function $\log I_{2\Omega} = \log I_c + \log K_2 + \alpha \log V_0$ where α is the slope. Unknown α and K_2 were extracted as the parameters of the least square fitting. Slope α = 1.686 ± 0.012 is 16% less than theoretical value of 2.0 probably due to some small unaccounted contribution from the terms in $I(t)$ proportional to even powers of V_0 greater than 2. Using the obtained parameters K_2, V_π and δ_c, we then evaluated previously unknown E-O coefficient r_{63}. Assuming that coefficients r_{61} and r_{63} were of the same order of magnitude, we could neglect the first term in Eq. (50) as small (approximately 16 times smaller) comparing to the second term. With this in mind, we found from Eqs. (54) and (50) that $r_{63} \approx 1.05$ pm/V, two orders of magnitude smaller than coefficients r_{12} and r_{22}.

6.3 *Optimum Angle of Incidence*

As is shown in Appendix B, the maximum amplitude I_Ω must be observed when the light propagates along axis z. This could be used to determine the orientation of axis z by purely E-O measurements without retaining to the second harmonic generation (SHG) method.[14] The advantage of this approach is that it does not need an additional

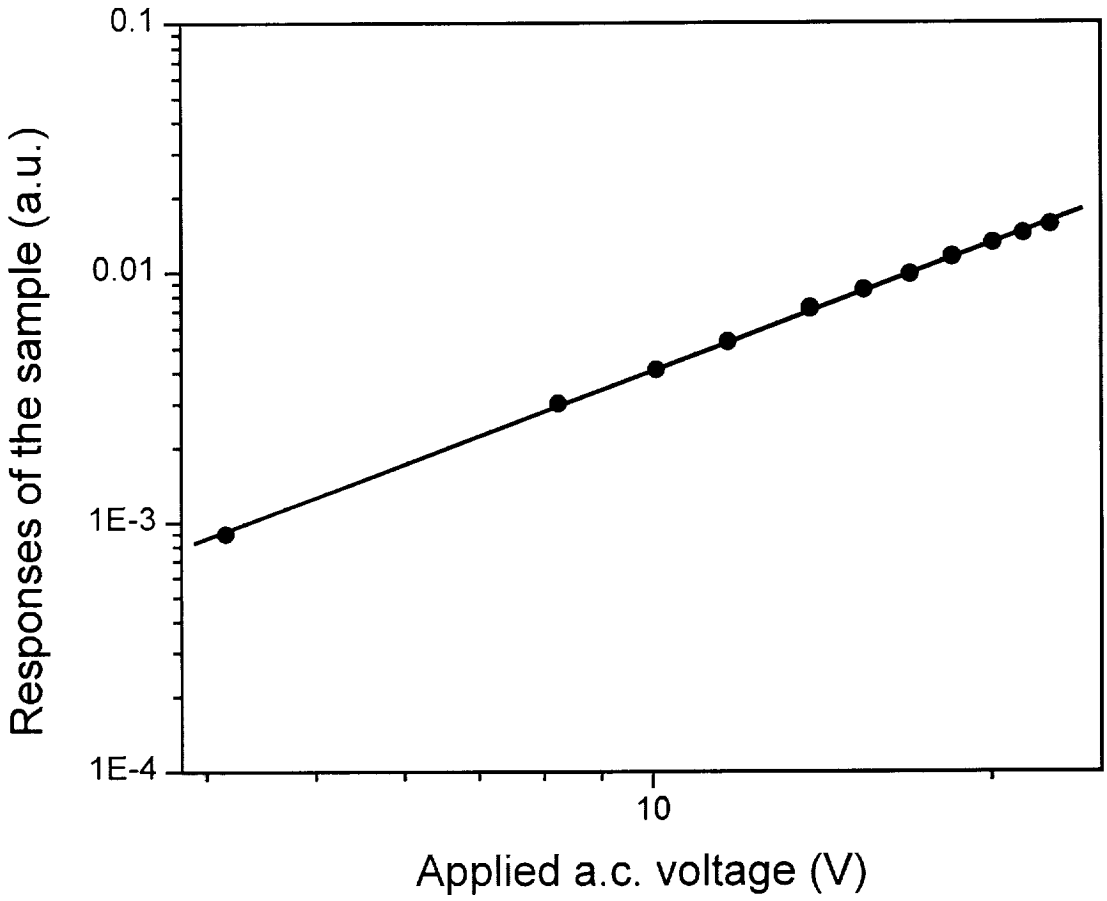

Fig. 9. The double frequency response of the sample versus the a.c. voltage. The fundamental frequency was 13.5 kHz.

relatively powerful pulsed coherent source of infrared radiation such as Q-switched Nd: YAG laser that brings up a potential risk of damaging the sample.

The orientation of axis z was found by performing the following operations with the sample while keeping the direction of the light beam fixed (Fig. 10). First, we rotated the sample around the beam (horizontal axis) and set certain angle θ between the cracks and direction P_1. Second, we tilted the sample around vertical axis or, in other words, scanned angle φ between the normal to the film and the vertical plane defined by the beam and P1. Angle φ was also the angle of incidence of the light beam. During the scan we measured amplitude I_Ω of intensity at fundamental frequency. Maximum amplitude I_Ω corresponded to optimum angle $\varphi_{opt}(\theta)$. While tilting the sample, we always monitored the position of the beam in the sample with a microscope. Some correcting shift was added to the sample in order to return the beam back to its initial position in the film and thus to exclude any signal variation due to the beam displacement. It is seen in Fig. 10 that at some orientation of the sample θ_1 axis z, which is not normal to the film, can be brought to the vertical plane. Maximum projection of axis z on the direction of the beam and, correspondingly, maximum amplitude I_Ω of the signal are reached at angle $\varphi_{opt}(\theta_1) = 0$ (the beam is perpendicular to the film at this incidence angle). By rotating the sample at 90^0 ($\theta_2 = \theta_1 + 90^0$), we can bring axis z to the horizontal plane made by the beam and P2. Then by tilting the film we can make z parallel to the beam and gain maximum of amplitude I_Ω. The corresponding angle $\varphi_{opt}(\theta_2)$ must be the largest possible. If we orient the sample at angle θ_3 that satisfies condition $\theta_1 < \theta_3 < \theta_2$, the corresponding angle $\varphi_{opt}(\theta_3)$ must be $0 < \varphi_{opt}(\theta_3) < \varphi_{opt}(\theta_2)$.

Fig. 11 shows amplitude I_Ω plotted versus angle φ at three different angles: $\theta_1 \approx 45^0$, $\theta_2 \approx 45^0+90^0=135^0$, and $\theta_3 \approx 60^0$. Each experimental plot has its maximum at a different optimum angle $\varphi_{opt\ i}(\theta_i)$. In good agreement with the previous discussion, we had $0 \approx \varphi_{opt}(\theta_1) < \varphi_{opt}(\theta_3) < \varphi_{opt}(\theta_2)$.

Fig. 10b shows that angle ξ can be linked to $\varphi_{opt}(\theta_2)$ by the Snell's law

$$\sin\varphi_{opt}(\theta_2) = n'(\theta_2)\sin\xi, \tag{63}$$

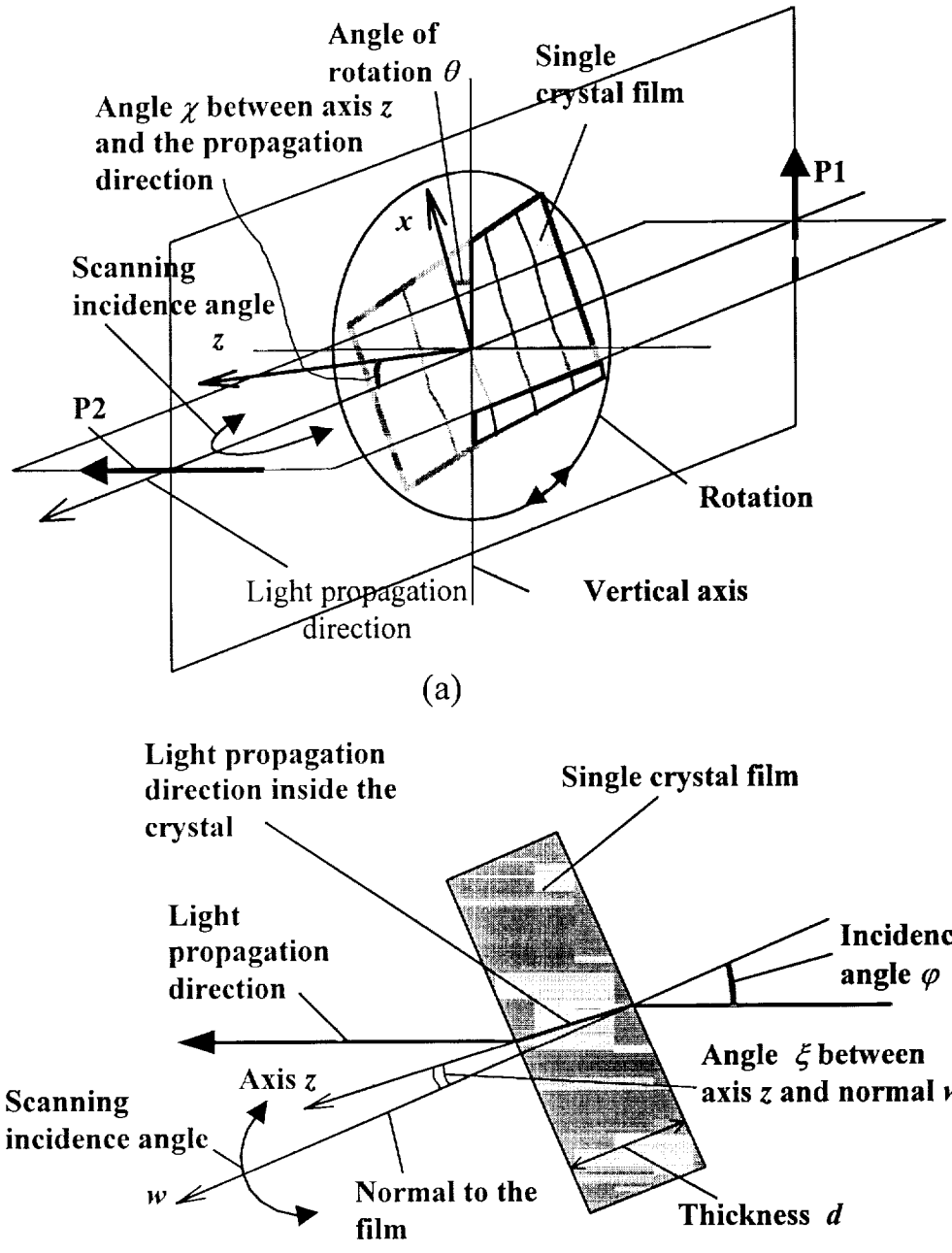

Fig. 10. The orientation of the dielectric axes with respect to the thin film. The dielectric axis z has an angle of nearly 5^0 to the normal to the thin film plane.

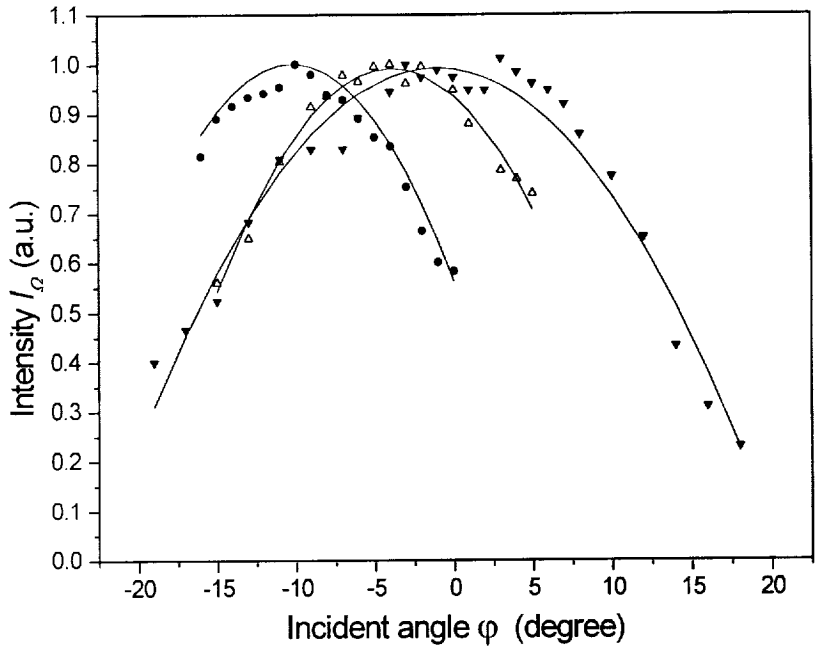

Fig. 11. The response of the sample versus the incidence angle φ at $\theta = 135^0$ (solid circles), $\theta = 45^0$ (solid reversed triangles), $\theta = 60^0$ (open triangles). Solid lines represent the results of fitting experimental data with parabola. Each data set was normalized by its maximum.

where $n'(\theta_2)$ is the effective refractive index of the crystal for the incident vertically polarized optic field determined as

$$n'(\theta_2) = (\cos^2\theta_2/n_x^2 + \sin^2\theta_2/n_y^2)^{-1/2} \quad (64)$$

Experimental plot $\varphi_{opt}(\theta)$ (Fig. 12) was approximated by function described by Eqs. (63) and (64) with ξ as a parameter of fitting. Angle ξ was found to be $(5.2 \pm 0.2)^0$.

7. Design of an electro-optic modulator

We also explored the possibility of making a thin film waveguide E-O modulator integrated with coupling prisms. The thin film should be able to accommodate two modes: mode 0 and mode 1 (Fig. 13). A light beam is injected into the film. At the output side, two beams corresponding to mode 0 and mode 1 are decoupled from the waveguide by prism coupler 2'. They are recombined by lens 5'. Interference fringes appear on screen 7. Fiber transfers the intensity of the pattern in a fixed location on the screen to detector 8. If we apply voltage to electrodes 3 and 3', transverse E-O modulation will produce a shift of the interference pattern. The ratio of the travel length of the light to the thickness of the film is of the order of 1000, so the driving voltage can be as low as 3.26 V. Fig. 14 shows the photograph of an experimental prototype of the system with TM traveling mode.

The main design problem is to attach the high index prism to the substrate maintaining the gap between them less than a fraction of micron. There also has to be no step between the top face of each prism and the substrate. We found that it is difficult to satisfy these conditions by attaching the prisms with various optical glues. Welding prisms to the substrate completely different thermal expansion properties also seems inefficient: it may result into cracking the prisms and the substrate or breaking them apart during the process of cooling after the welding is complete. The work on the design needs to be continued.

8. Conclusions

We developed the plate-guided method of growing single crystal films of NPP with uniform areas as large as 0.25 mm^2. The half-wave voltage of the E-O modulation and the figure-of-merit were obtained by using the a.c. modulation technique. The E-O effect is pseudo longitudinal since the configuration of the experiment is that of a longitudinal intensity modulator but the main contribution to the effect originates from the transverse component of the electric field. The orientation of dielectric axis z was determined by measuring the maximum amplitude of the modulated intensity of the transmitted light when varying the incidence angle of the light beam. The E-O coefficients r_{12}, r_{22} have been evaluated as 461 pm/V and 154 pm/V respectively. Assuming that coefficients r_{61} and r_{63} were of the same order of magnitude, we found them to be two orders of magnitude less than r_{12} and r_{22}. Thin single crystal films of NPP appeared to be suitable to various applications such as longitudinal E-O modulators (for instance, in the configuration of Fabry-Perot interferometer) and optical switches.

We designed of the electro-optic modulator based on a single crystalline film of organic material NPP has been explored. The problems of building a version of the modulator integrated with prism coupler have been identified. Preliminary testing of thin film waveguide prototype of the modulator has been performed.

We performed the evaluation of the figures-of merit of the electro-optic modulator has been performed. It is based on the characterization of the electro-optic properties of the films using the longitudinal intensity modulation technique with low (of the order of 10 V) alternating driving voltage. Both the fundamental and double frequency responses were used for the characterization. The electro-optic effect was pseudo longitudinal since the configuration of the experiment was that of a longitudinal intensity modulator but the main contribution to the effect originates from the transverse component of the external electric field. By purely electro-optic means we determined the orientation of the dielectric axes and measured the half-wave voltage, the figure-of-merit, and electro-optic coefficients r_{12} and r_2 to be 3.24 kV, 99.2 pm/V, 461 pm/V, and 154 pm/V respectively. We also found that electro-optic coefficients r_{61} and r_{63} were two orders of magnitude less than r_{12} and r_2. Respectively, the driving voltage of the

modulator in the transverse waveguide configuration would be 3.24 V (the length of the waveguide is assumed to be 10 mm and the thickness of the single crystal film – 10 μm). The extinction ratio of the experimental modulator in the pseudo longitudinal configuration (Fig. 7) was approximately 8.4 dB, slightly less than expected. The improvement of the extinction ratio could be expected in the next generation of the modulator with higher optical quality of the single crystal films grown.

Based on the results of characterization of the figures-of merit, we made the conclusion that the modulator based on a thin film of NPP is feasible and has a great potential of being used in optic communication with a modulation bandwidth of up to 100 GHz and a driving voltage of the order of 3 to 5 V.

Comparison of the objectives and the achievements showed that all the objectives of the project outlined in the initial proposal have been met.

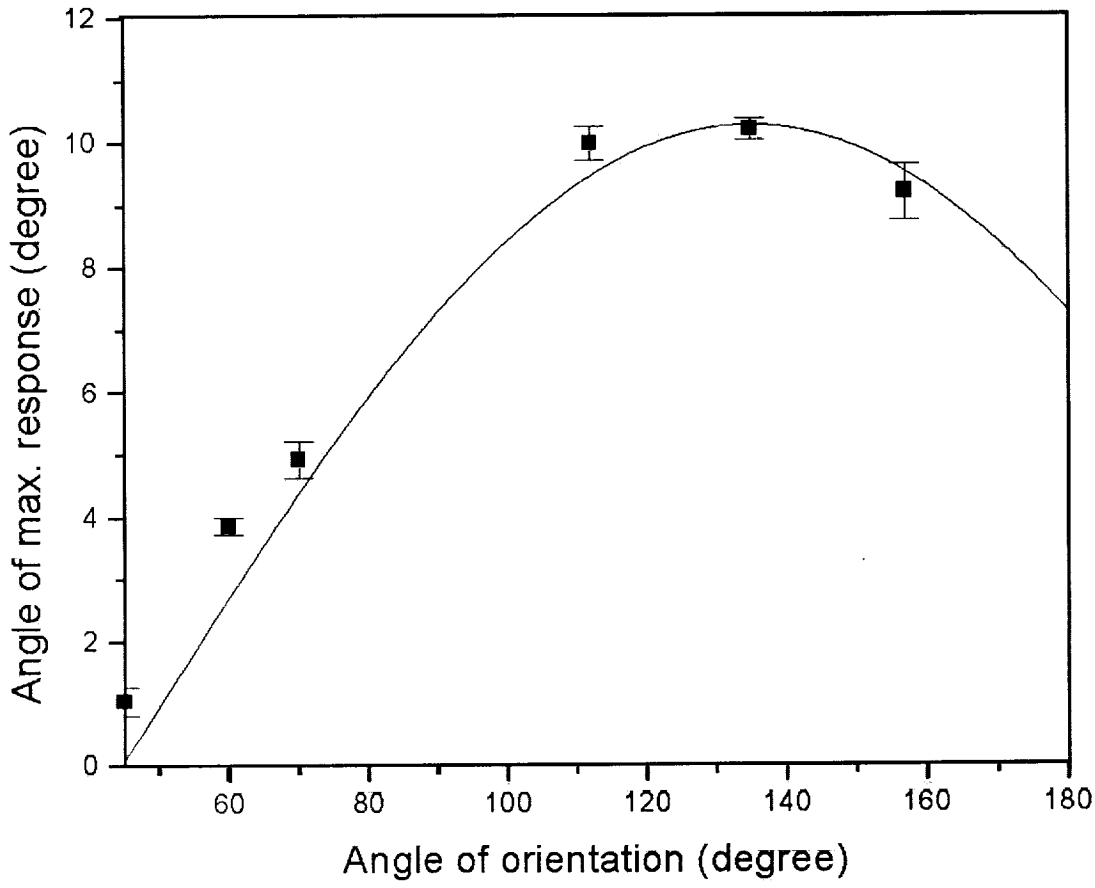

Fig. 12. Angle φ_{opt} of maximum response of the sample versus angle θ of orientation of the crystal. Solid line represents fitting.

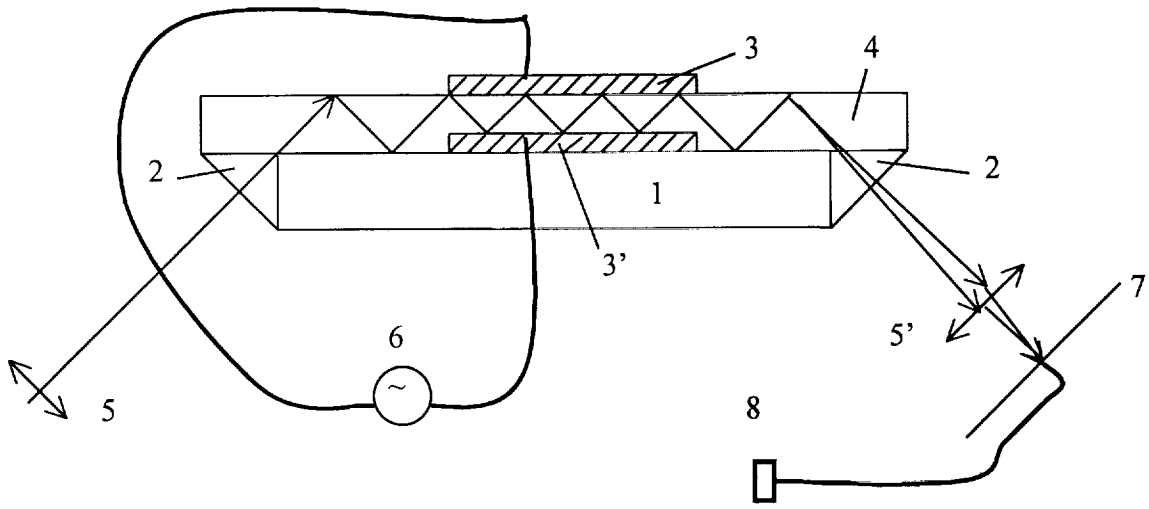

Fig. 13. Thin film waveguide E-O modulator integrated with coupling prisms. Element 1 is the fused quartz substrate, 2 and 2' are the high index glass prisms, 3 and 3' are conducting layers, 4 is the organic thin film, 5 and 5' are lenses, 6 is the modulating signal, 7 is the interference plane used to observe fringe patterns, 8 is the detector.

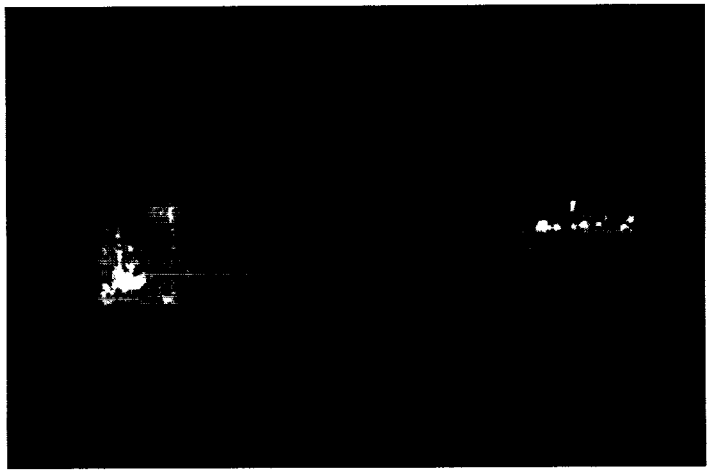

Fig. 14. Experimental thin film waveguide integrated with coupling prisms. TM traveling mode is shown.

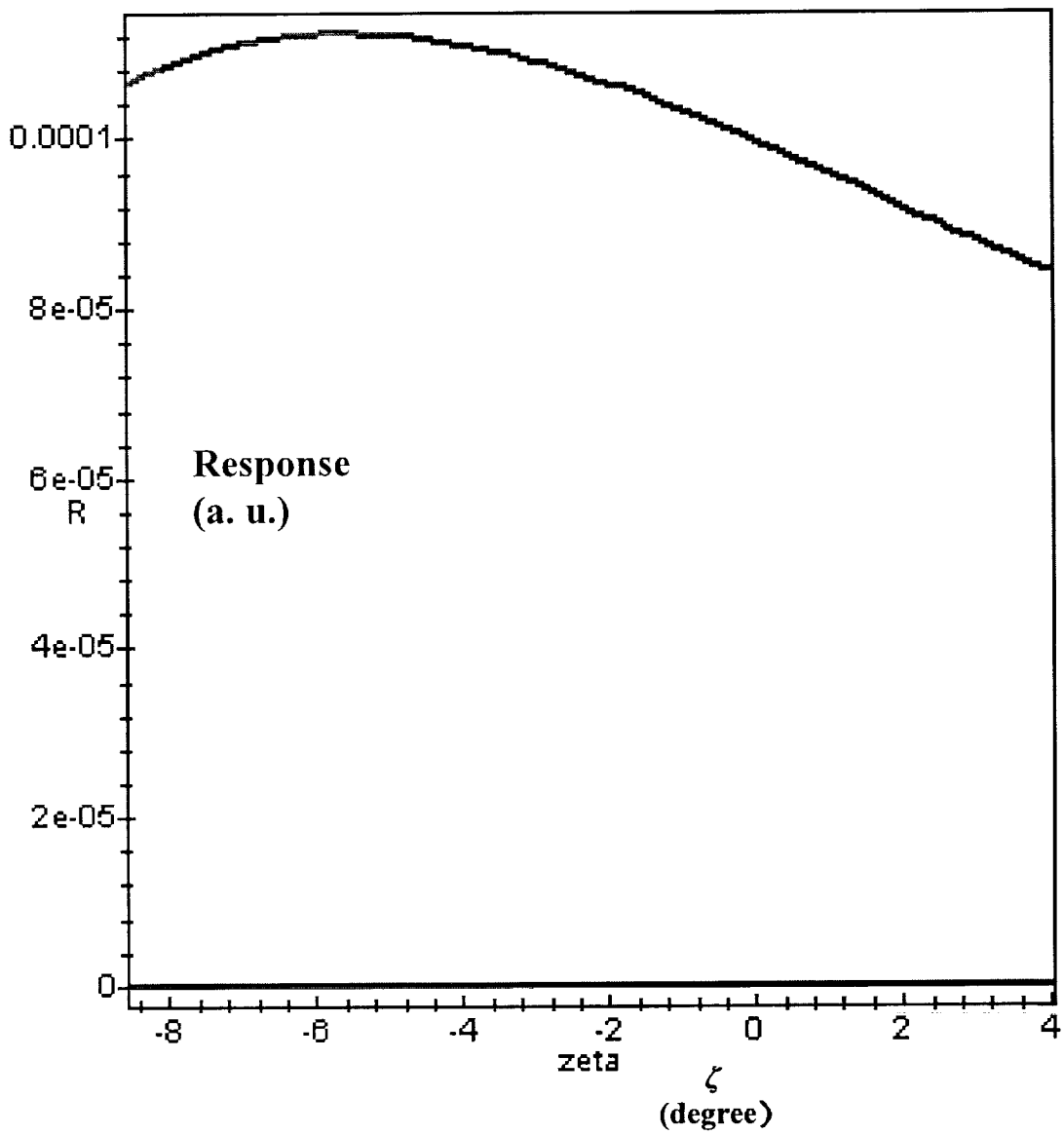

Fig. 15. The results of theoretical simulations of the response of the sample plotted against the incidence angle of light within the crystal.

9. References

1. J. Badan, R. Hierle, A. Perigaud, and J. Zyss, "Nonlinear organic crystals: theoretical concepts, materials, and optical properties," ACS Symp. Ser. 233, 81-107 (1983).
2. G. F. Lipscomb, A. F. Garito, and R. S. Narang, "An exceptionally large linear electro-optic effect in the organic solid MNA," J. Chem. Phys. **75**, 1509-1516 (1981).
3. Jianjun Xu, Ligui Zhou, and M. Thakur, "Measurement of electro-optic effects in single crystal films of N-(4-nitrophenyl)-L-prolinol," Appl. Phys. Lett. **69**, 1197-1198 (1996).
4. F. Pan, G. Knopfle, Ch. Bosshard, S. Follonier, R. Spreiter, M. S. Wong, and P. Gunter, "Electro-optic properties of the organic salt 4-N, N-dimethylamino-4'-N'-methyl-stilbazolium tosylate," Appl. Phys. Lett. **69**, 13-15 (1996).
5. J. Zyss, J. F. Nicoud, and M. Coquillay, "Chirality and hydrogen bonding in molecular crystals for phase-matched second-harmonic generation: N-(4-nitrophenyl)-(L)-prolinol (NPP)," J. Chem. Phys. **81**, 4160-4167 (1984).
6. H. S. Nalwa, T. Watanabe, and S. Miyata, "Organic materials for second-order nonlinear optics," in *Nonlinear optics of organic molecules and polymers*, H. S. Nalwa and S. Miyata, Eds. (CRC Press, New York, 1997), pp. 248-249, 136-137.
7. J. Zyss and D. S. Chemla, "Quadratic nonlinear optics and optimization of the second-order nonlinear optical response of molecular crystals," in *Nonlinear optical properties of organic molecules and crystals,* D. S. Chemla and J. Zyss, Eds. (Academic Press, Orlando, Florida, 1987), Vol. 1, pp. 155-159.
8. B. Yu. Shekunov, E. E. A. Shepherd, J. N. Sherwood, and G. S. Simpson, "Growth and perfection of organic nonlinear optical materials- kinetics and mechanism of the growth of N-(4-nitrophenyl) prolinol (NPP) crystals from methanol and toluene solution," J. Phys. Chem. **99**, 7130-7137 (1995).
9. A. Leyderman, M. Espinosa, T. Timofeeva, R. Clark, D. Frazier, and B. G. Penn, "Growth and characterization of crystalline films of meta-nitroaniline (mNA) and

2-cyclo-octylamino-5-nitropyrydine (COANP)," in *Space processing of materials*, N. Ramachandran, Ed., Proc. SPIE **2809**, 144-154 (1996).

10. A. Leyderman, " Organic crystalline films for optical applications and related methods of fabrications," US Patent 5746823, May (1998).
11. A. Leyderman, " Organic crystalline films for optical applications and related methods of fabrications," US Patent 6198530, March (2001).
12. T. Yoshimura, "Characterization of the electro-optic effect in styrylpyridinium cyanine dye thin-film crystals by an ac modulation method," J. Appl. Phys. **62**, 2028-2032 (1987).
13. M. V. Klein and T. E. Furtak, Optics, 2nd Edition, John Wiley & Sons, New York, 1986, pp. 637-639, 641.
14. I. Ledoux, D. Josse, P. Vidakovic, and J. Zyss, " Highly efficient single-crystalline organic thin films for quadratic nonlinear optics", Opt. Eng. **25**, 202-210 (1986).

Appendix A. E-O effect in the case when dielectric axis *Y* lies in the plane of the film

When voltage $V_a(t)$ is applied to the electrodes, the external electric field $\mathcal{E}$ created by the voltage is normal to the film. We assume that the two-fold dielectric axis y is within the plane of the film. This means that component $\mathcal{E}_y$ of the external electric field will be equal to zero. Putting $\mathcal{E}_y = 0$ in Eq. (28) makes $e_0=0$. Correspondingly, in Eq. (48) amplitude I_Ω becomes zero. It means that at angle $\theta \approx 45^0$, at which we oriented the sample in the experiment, there should be no signal $I(t)$ at frequency Ω of the alternating voltage $V_a(t)$ (no linear E-O effect). Opposite to this, we observed strong response of the sample at fundamental frequency Ω. This requires the two-fold axis y to lie off the plane of the film.

Appendix B: The dependence of the E-O response on the angle between dielectric axis *z* and the direction of light propagation

For a biaxial crystal, there are two optical axes, and both of them are located within x-z plane. If the light propagates along the optic axis, it will not experience natural birefringence. Assuming the principal refractive indices have relation $n_x > n_y > n_z$ (as in NPP), we can determine β_1 and β_2, the angles between axis x and the two optic axes, as (Ref. 13)

$$\tan\beta_{1,2} = \pm\frac{n_x}{n_z}\sqrt{\frac{n_y^2-n_z^2}{n_x^2-n_y^2}} \qquad \text{(B1)}$$

In our case $\beta_1 = 62.5^0$ and $\beta_2 = -62.5^0$. Two optic axes have angles $\alpha_1 = 90^0 + \beta_2 = 27.5^0$ (see Fig. B1) and $\alpha_2 = 90^0 + \beta_1 = 152.5^0$ with dielectric axis z respectively. Assuming γ_1, γ_2 are the angles between the light propagation direction $\boldsymbol{k}$ (with components k_x, k_y, k_z) and two optical axes, we have

$$\cos\gamma_1 = \frac{k_x \sin\alpha_1}{k} + \frac{k_z \cos\alpha_1}{k}, \tag{B2}$$

$$\cos\gamma_2 = \frac{k_x \sin\alpha_2}{k} + \frac{k_z \cos\alpha_2}{k}, \tag{B3}$$

where $k_x = \cos\theta\sin\chi$, $k_y = \sin\theta\sin\chi$, $k_z = \cos\chi$, k is the magnitude of vector $\boldsymbol{k}$, angle θ is the previously introduced angle between axis x and the polarization direction of polarizer P_1, angle χ is the angle between axis z and the light propagation direction within the crystal. Angle χ is linked to angle ζ of refraction of the incident light beam within the crystal ζ by equation

$$\cos\chi = \sin\xi \sin 45^0 \sin\zeta (\sin\theta - \cos\theta) + \cos\xi\cos\zeta. \tag{B4}$$

The two refractive indices corresponding to propagation direction $\boldsymbol{k}$ can be described as

$$\frac{1}{n_a^2} = \frac{1}{2}\left[\frac{1}{n_z^2} + \frac{1}{n_x^2} + \left(\frac{1}{n_z^2} - \frac{1}{n_x^2}\right)\cos(\gamma_1 + \gamma_2)\right], \tag{B5}$$

$$\frac{1}{n_b^2} = \frac{1}{2}\left[\frac{1}{n_z^2} + \frac{1}{n_x^2} + \left(\frac{1}{n_z^2} - \frac{1}{n_x^2}\right)\cos(\gamma_1 - \gamma_2)\right]. \tag{B6}$$

The distance, which the light travels within the crystal, can be described as

$$d' = d/\cos\zeta, \tag{B7}$$

Then we assume that the external a.c. electric field is applied to the film. There will be electric field induced changes in n_a and n_b and the rotation of the ellipse of refractive indices. Making steps similar to those described by Eqs. (24) through (48), we can eventually arrive to the relation

$$I_{\Omega}(\zeta,\ \theta) \propto \sin[\delta_c \cos^{-1}\zeta]\sin^2 2\theta \cos^{-1}\zeta V_0 . \qquad \text{(B8)}$$

Function $I_{\Omega}(\zeta,\ \theta)$ in Eq. (B8) was simulated numerically for various angles ζ and θ. At angle $\theta = 135^0$, when axis z lies in the horizontal plane made by the light beam and P2, amplitude I_{Ω} reaches its absolute maximum when $\zeta = \xi$ as is shown in Fig. 15. This means that the maximum linear E-O effect must be observed when the light beam is parallel to axis z.

An additional proof of the conclusion derived from the results of the numerical simulations was obtained experimentally from the observation of the so called "cats eye" pattern produced by a scattered light beam diffracted on the crystal.

Appendix C. List of publications related to the project

1. Alexander Leyderman, Yunlong Cui, Javier Wu Li, Sergey Sarkisov, Michael Curley, Curtis Banks, Benjamin Penn, "Growth and characterization of single crystal organic thin films for electro-optic modulators," in *Operational Characteristics and Crystal Growth of Nonlinear Optical Materials,* Ravindra B. Lal, Donald O. Frazier, Editors, Proceedings of SPIE Vol. 3793, 45-54 (1999).
2. Zhifu Liu, Sergey S. Sarkisov, Maichael J. Curley, Alexander Leyderman, Yulong Cui, Javier Wu Li, and Benjamin Penn, "Diagnostics and growth of organic thin films for electro-optic modulators with low driving voltage," In *Optical Devices and Diagnostics in Material Science*, D.L. Andrews, T. Asakura, S. Jutamulia, W.P.Kirk, M.G. Lagally, R.B. Lal, J.D. Trolinger, Editors, Proceedings of SPIE Vol. 4098 (2000) 40-51.
3. Sergey Sarkisov, Zhifu Liu, Michael Curley, Curtis Banks, "Organic and inorganic crystals for electro-optic modulators with low driving voltage," V.V. Shepelevich, N.N. Egorov, Editors, Proceedings of SPIE Vol. 4358, 153-164 (2001).

4. Zhifu Liu, S.S. Sarkisov, M.J. Curley, A. Leyderman, Yulong Cui, J.W. Li, B.G. Penn,"Longitudinal electro-optic effect in single crystal films of N-(4-nitrophenyl)-(L)-prolinol (NPP)," in OSA *Trends in Optics and Photonics (TOPS) Vol. 56, Conference on Lasers and Electro-Optics (CLEO 2001),* Technical Digest, Postconference Edition (Optical Society of America, Washington DC, 2001), p. 296.
5. Zhifu Liu, Sergey S. Sarkisov, Michael J. Curley, Alexander Leyderman, Javier W. Li, and Charles Y. Lee, "Electro-optic modulators based on organic single crystal films," in *Linear and Nonlinear Optics of Organic materials,* Manfred Eich, Mark G. Kuyk, Editors, Proceedings of SPIE Vol. 4461 (2001) 260-271.
6. Zhifu Liu, S.S. Sarkisov, M.J. Curley, A. Leyderman, Yulong Cui, J.W. Li, and B.G. Penn, Pseudo longitudinal electro-optic effect in single crystal films of N-(4-nitrophenyl)-(L)-prolinol (NPP), Submitted to JOSA B.

Appendix D. List of graduate students supported by NASA Grant NAG8-1498

7. Curtis Banks (Ph.D. Physics)
8. Darnell Diggs (Ph.D. Physics, Graduated in July, 2001, now is a research staff member at the AFOSR Research Lab, Wright Patterson Air force Base)
9. Zhifu Liu (Ph.D. Physics, Graduated in July, 2001, now is a postdoctoral research fellow at the North Western University, Evanston, IL)
10. Aisha Fields (Ph.D. Physics)
11. William Omereji (M.S. Physics)
12. Daniel Wilson (M.S. Physics)